

# Imaging of Freeze-Fractured Cells with in Situ Fluorescence and Time-of-Flight Secondary Ion Mass Spectrometry

Thomas P. Roddy, Donald M. Cannon, Jr., Chad A. Meserole, Nicholas Winograd, and Andrew G. Ewing\*

152 Davey Laboratory, Department of Chemistry, Pennsylvania State University, University Park, Pennsylvania 16802

**Bioanalytical imaging techniques have been employed to investigate cellular composition at the single-cell and subcellular regimes. Four imaging modes have been performed sequentially in situ to demonstrate the utility of a more integrated approach to imaging cells. The combination of bright-field, scanning ion, and fluorescence microscopy complements TOF-SIMS imaging of native biomolecules. Bright-field microscopy provides a blurred visualization of cells in frozen-hydrated samples, while scanning ion imaging provides a morphological view of freeze-fractured cells after TOF-SIMS analysis is completed. With the use of selective fluorescent labels, fluorescence microscopy allows single mammalian cells to be located in the complex ice matrix of freeze-fractured samples, a task that has not been routine with either bright-field or TOF-SIMS. A fluorescent label, DiI ( $m/z$  834), that does not interfere with the mass spectra of membrane phosphatidylcholine, has been chosen for fluorescence and TOF-SIMS imaging of membrane phospholipids. In this paper, in situ fluorescence microscopy allows the distinction of single cells from ice and other sample debris, previously not possible with bright-field or scanning ion imaging. Once cells are located, TOF-SIMS imaging reveals the localization of membrane lipids, even in the membrane of a single 15- $\mu\text{m}$  rat pheochromocytoma cell. The utility of mapping lipids in the membranes of single cells using this integrated approach will provide more understanding of the functional role of specific lipids in functions of cellular membranes.**

Knowledge of the structure of cell membranes is crucial to understanding their function. In this regard, the fluid mosaic model of lipid motion within cellular membranes has come under scrutiny in recent years.<sup>1–4</sup> This is in part because fluorescence imaging techniques have been used to demonstrate the existence of chemical domains in cells and to observe chemical domains spontaneously developing in liposomes.<sup>5–8</sup> Furthermore, the

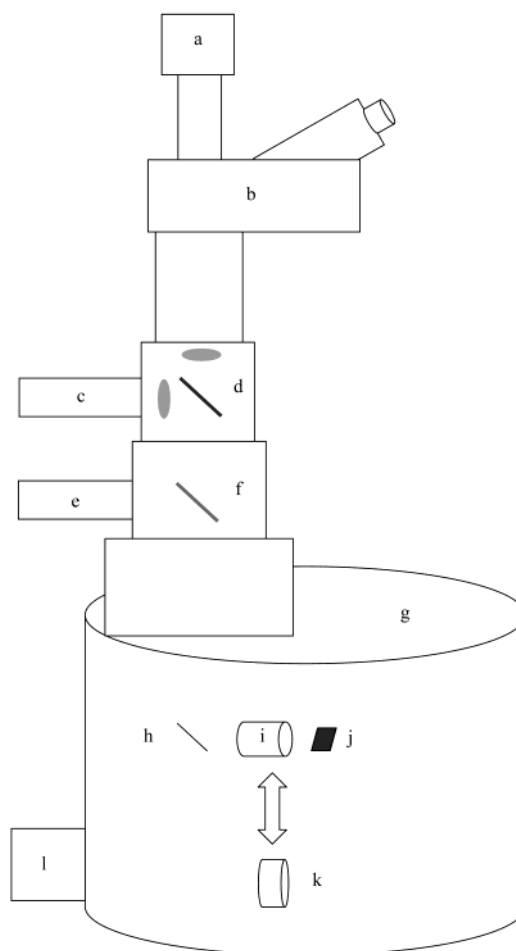


Figure 1. Schematic of imaging apparatus used to collect epifluorescence, reflected bright-field, secondary ion, and scanning ion images: (a) camera, (b) trinocular microscope head, (c) 100-W Hg source, (d) fluorescence filter set, (e) 50-W halogen source, (f) 50% transmittance mirror, (g) analysis chamber, (h) 100% reflectance mirror, (i) objective, (j) sample, (k) SIMS extraction lens and channeltron, and (l) TOF mass analyzer.

curvature model of lipid packing leads to the concept that differently shaped membranes will contain unique lipid compo-

\* To whom correspondence should be addressed. E-mail: age@psu.edu. Fax: (814) 863-8081.

(1) Kobayashi, T.; Storrie, B.; Simons, K.; Dotti, C. G. *Nature* **1992**, *359*, 647–650.

(2) Nelson, W. J. *Science* **1992**, *258*, 948–955.

(3) Glaser, M. *Curr. Opin. Struct. Biol.* **1993**, *3*, 475–481.

(4) Singer, S. J.; Nicolson, G. L. *Science* **1972**, *175*, 720–731.

(5) Glaser, M.; Rodgers, W.; Luan, P.; Yang, L.; Wang, F. *Biophys. J.* **1993**, *64*, A247–A247.

(6) Simons, K.; Ikonen, E. *Nature* **1997**, *387*, 569–572.

(7) Bagatolli, L. A.; Gratton, E. *Biophys. J.* **2000**, *78*, 290–305.

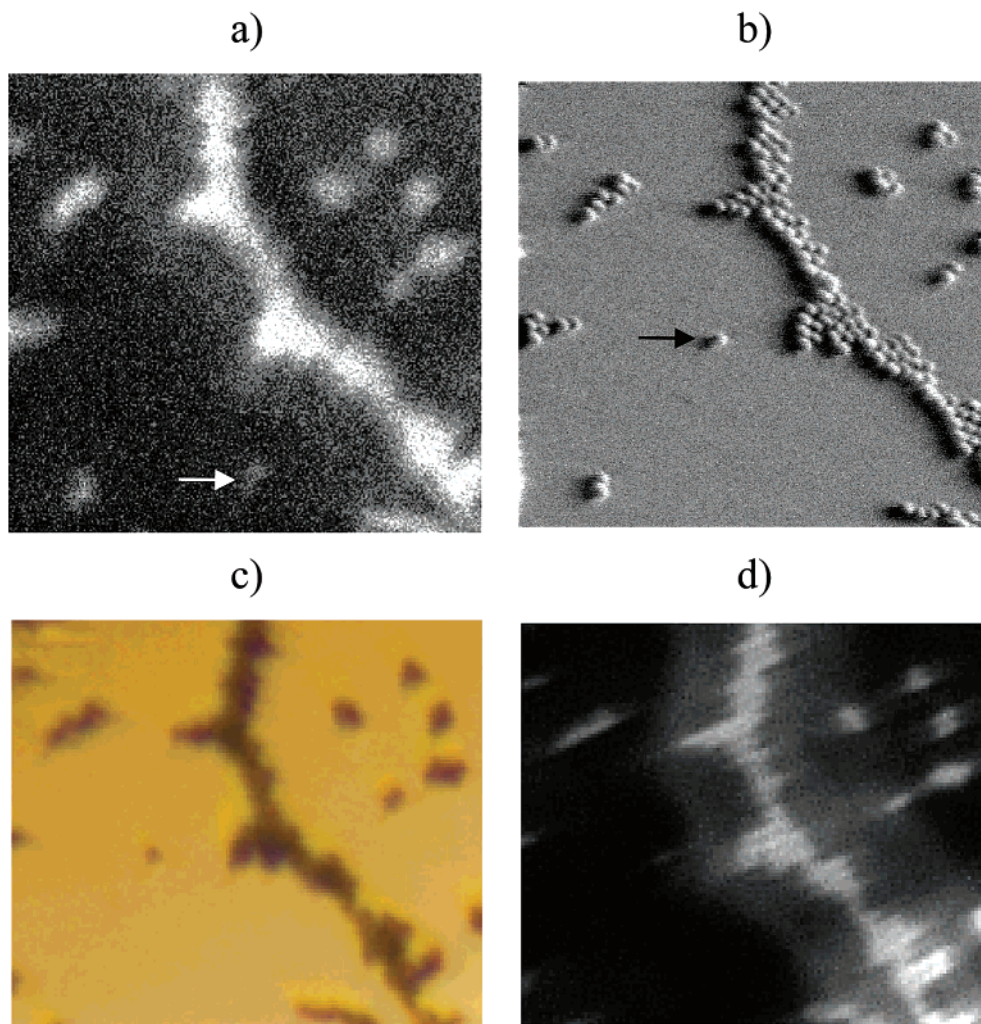


Figure 2. Images of 3- $\mu\text{m}$  red fluorescent beads dried onto a silicon substrate using the four in situ imaging techniques ( $\sim 120\text{-}\mu\text{m}$ -wide field of view): (a) molecule-specific TOF-SIMS of  $[\text{C}_5\text{H}_6]^+$  hydrocarbon, (b) scanning ion, (c) reflected bright field, and (d) epifluorescence. The arrows indicate a bead that moved across the surface during scanning ion imaging.

nents.<sup>9</sup> These findings indicate that the chemical makeup of lipid domains in cells with highly active membranes is important in regulating function (e.g., exocytosis). Further investigation that spatially targets lipid heterogeneity at the single-cell level is required to understand the relation between phospholipid domains and their function.

Imaging secondary ion mass spectrometry (SIMS) is an emerging tool for the study of the distribution of chemical species in tissues and cells.<sup>10–13</sup> To preserve chemical integrity during the in vacuo analyses required by mass spectrometry, samples are typically fixed, fractured, and freeze-dried prior to assay.<sup>14</sup>

- (8) Kurlach, J.; Schwille, P.; Webb, W. W.; Feigenson, G. W. *Proc. Natl. Acad. Sci. U.S.A.* **1999**, *96*, 8461–8466.
- (9) Yeagle, P. *The Membranes of Cells*, 2nd ed.; Academic Press: San Diego, 1993.
- (10) Chandra, S.; Ausserer, W. A.; Morrison, G. H. *J. Cell Sci.* **1992**, *102*, 417–425.
- (11) Morrison, G. H.; Gay, I.; Chandra, S. *Scanning Microsc. Suppl.* **1994**, *8*, 359–370.
- (12) Todd, P. J.; McMahon, J. M.; Short, R. T.; McCandlish, C. A. *Anal. Chem.* **1997**, *69*, 529A–535A.
- (13) Pacholski, M. L.; Cannon, D. M., Jr.; Ewing, A. G.; Winograd, N. *Rapid Commun. Mass Spectrom.* **1998**, *12*, 1232–1235.
- (14) Chandra, S.; Smith, D. R.; Morrison, G. H. *Anal. Chem.* **2000**, *72*, 104A–114A.

Chandra et al. utilized these sample preparation techniques with dynamic SIMS to image the localization of boron in brain tissue for neutron capture therapy studies.<sup>11,14,15</sup> Recently, the same group has shown subcellular localization of elements including boron in single human glioblastoma cells.<sup>16</sup> Static SIMS, a surface analysis method, allows the detection of relatively complex molecular ions when compared to dynamic SIMS, including various phospholipid molecular ions and their fragments.<sup>17</sup> McMahon et al. used static SIMS to show that phosphocholine, a major fragment of phosphatidylcholine, is clearly localized in air-dried sections of mouse brains.<sup>18</sup> Phospholipids have not been investigated at the subcellular level with SIMS to probe phospholipid diversity across the surface of individual cells.

Imaging phospholipids in single cells with static SIMS presents new challenges as fixing, slicing, and freeze-drying samples perturbs the submicrometer localization of molecules at the cell

- (15) Smith, D. R.; Chandra, S.; Coderre, J. A.; Morrison, G. H. *Cancer Res.* **1996**, *56*, 4302–4306.
- (16) Chandra, S.; Lorey, D. R., 2nd. *Cell Mol. Biol.* **2001**, *47*, 503–518.
- (17) Vickerman, J. C.; Briggs, D.; Henderson, A. *The Wiley Static SIMS Library*; Wiley: Chichester, 1996.
- (18) McMahon, J. M.; Short, R. T.; McCandlish, C. A.; Brenna, J. T.; Todd, P. J. *Rapid Commun. Mass Spectrom.* **1996**, *10*, 335–340.

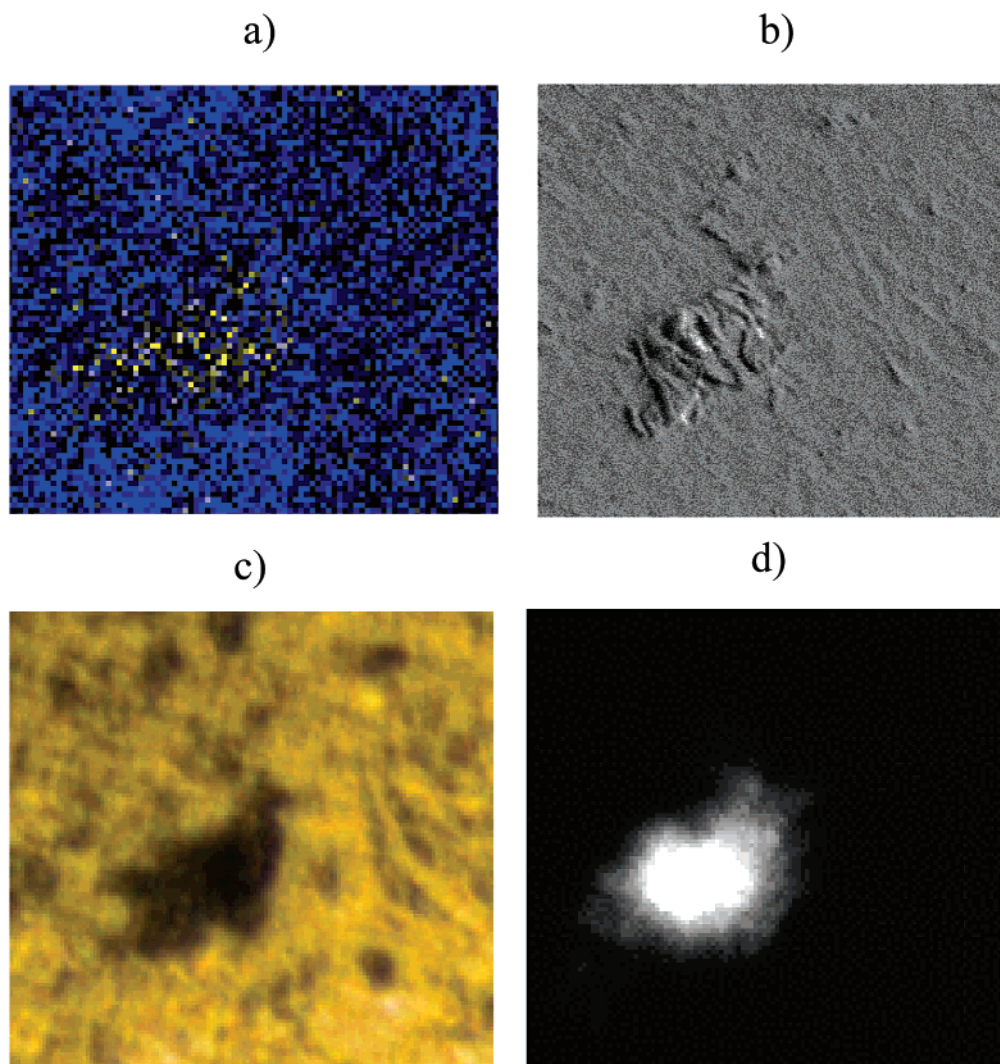


Figure 3. Images of NGF treated PC12 cells using the four in situ imaging techniques ( $\sim 120\text{-}\mu\text{m}$ -wide field of view): (a) molecule-specific TOF-SIMS image of water ( $m/z$  18) in blue on a scale of 0–3 counts and phosphocholine ( $m/z$  184) in yellow on a scale of 0–2 counts, (b) scanning ion, (c) reflected bright field, and (d) epifluorescence.

surface.<sup>19,20</sup> Preservation of chemical morphology is possible by rapid freezing of living samples in their native hydrated state. Freeze-fracture methods similar to those used in scanning electron microscopy have been modified to expose a fresh cellular surface for analysis in the ultrahigh vacuum environment of the SIMS instrument.<sup>13,19,21,22</sup> We have used TOF-SIMS to image elements and molecules, such as  $\text{Ca}^+$ ,  $\text{K}^+$ ,  $\text{H}_2\text{O}$ , DMSO, and cocaine in paramecia and phospholipids in red blood cells.<sup>13,22</sup> Cannon et al. have developed freeze-fracture methods to allow TOF-SIMS imaging of phospholipids in the membranes of two fusing liposomes.<sup>19</sup> In addition, neuronal-like rat pheochromocytoma cells (PC12) have been cultured onto SIMS substrates,<sup>23</sup> thus providing a single-cell model for TOF-SIMS imaging in neuroscience.

(19) Cannon, D. M.; Pacholski, M. L.; Winograd, N.; Ewing, A. G. *J. Am. Chem. Soc.* **2000**, *122*, 603–610.

(20) Ausserer, W. A.; Chandra, S.; Morrison, G. H. *J. Microsc.* **1989**, *154*, 39–57.

(21) Chandra, S.; Morrison, G. H.; Wolcott, C. C. *J. Microsc.* **1986**, *144*, 15–37.

(22) Colliver, T. L.; Brummel, C. L.; Pacholski, M. L.; Swaneck, F. D.; Ewing, A. G.; Winograd, N. *Anal. Chem.* **1997**, *69*, 2225–2231.

(23) Cannon, D. M.; Pacholski, M. L.; Roddy, T. P.; Winograd, N.; Ewing, A. G. *Secondary Ion Mass Spectrometry XII* **2000**, 931.

Although optical microscopy is the method of choice for imaging single cells in aqueous media, visualization of 12–15- $\mu\text{m}$ -diameter PC12 cells in the ice matrix of the freeze-fractured samples is difficult with this method. In this paper, we discuss the use of in situ bright-field and fluorescence microscopy to locate single fluorescently labeled cells in the fractured sample ice matrix. These cells are subsequently imaged with static TOF-SIMS and, with a diameter of only 15  $\mu\text{m}$ , are the smallest single cells imaged to date with this technique. The fragmentation and photobleaching characteristics of 1,1'-dioctadecyl-3,3',3'-tetramethylindocarbocyanine perchlorate (DiI) are also examined with TOF-SIMS. Adding scanning ion microscopy for morphological detail, this novel imaging scheme, combining four orthogonal techniques, is especially valuable in imaging single cells in freeze-fractured samples. To demonstrate the utility of the technique, we present TOF-SIMS images of lipids in the membrane of a single freeze-fractured PC12 cell.

## EXPERIMENTAL SECTION

**Secondary Ion Mass Spectrometry.** All analyses were performed in a Kratos (Manchester, U.K.) Prism TOF-SIMS



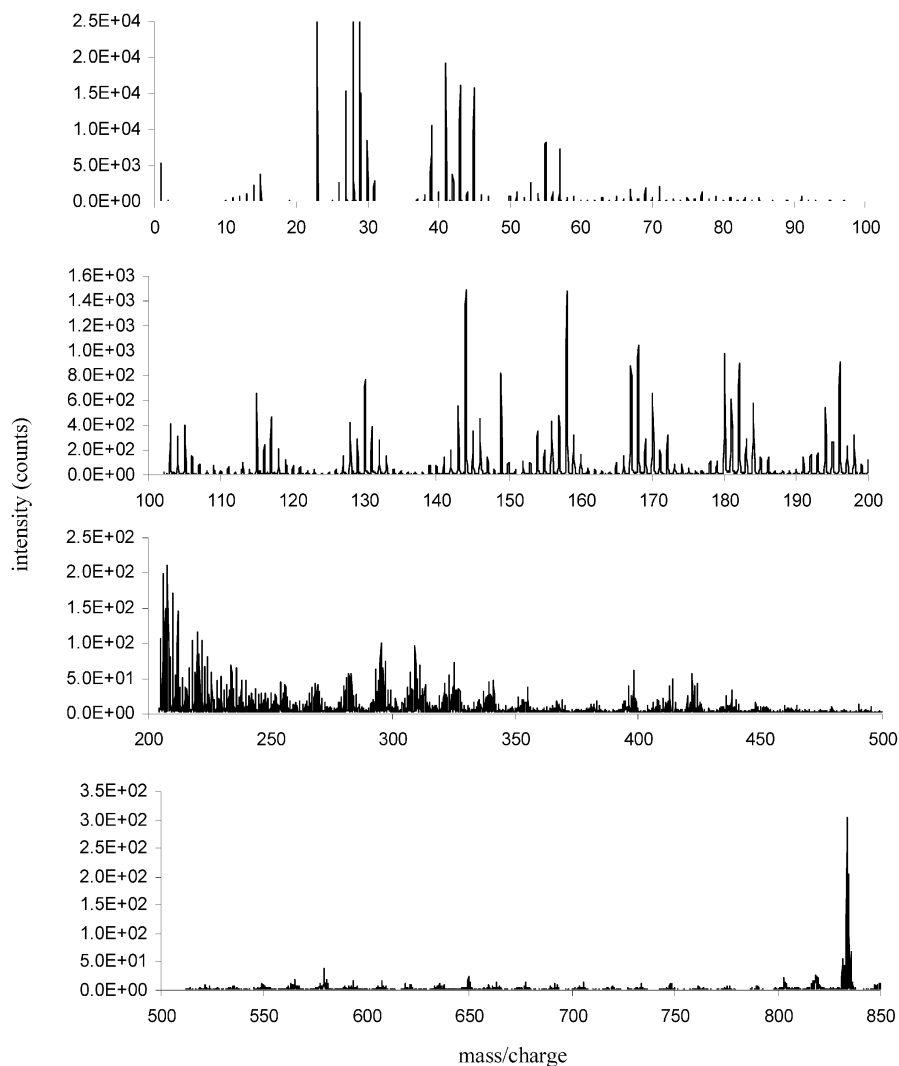


Figure 4. Positive TOF-SIMS spectrum of DiI standard on Si. Peaks at  $m/z$  834 correspond to the molecular ion of DiI. Peaks between at 410 and 424 are fragment ions (see Figure 5). The peak at  $m/z$  414 corresponds to a hydrolysis of DiI as discussed in the text. Peaks at 14  $m/z$  intervals are  $[M - C_nH_{2n}]^+$  ions.

spectrometer with a FEI (Beaverton, OR) gallium liquid metal ion gun (LMIG) with a 500-pA beam, 200-nm probe size, 25-kV beam voltage, and a 20–100-ns pulse width, oriented  $45^\circ$  to the sample. The liquid nitrogen ( $LN_2$ )-cooled stage (Kore Tech. Ltd., Cambridge, U.K.) was biased at  $\pm 2.5$  kV with an extraction lens biased at an opposite polarity of 4.7 kV. The horizontal time-of-flight path was 4.5 m in length including a reflectron. A microchannel plate assembly (Galileo Co., Sturbridge, MA) was used for detection. Mass resolution of this instrument was typically 4000 at  $m/z$  200 with 50% ion transmission efficiency. Spectra of standards were collected from a sample area of  $\sim 15\,000\ \mu\text{m}^2$ . The intensity of selected ions from the TOF mass spectrum was plotted in submicrometer pixels to generate an image. Spectra of freeze-fractured PC12 cells were obtained during imaging experiments and were collected across the same area as the imaged surface.

**Scanning Ion Imaging.** The instrument was also equipped with a channeltron detector (Burle, Lancaster, PA) positioned  $\sim 0.5$  cm from the sample to record scanning ion micrographs. The current of charged species and electrons emitting from the sample were monitored to generate a morphological image of the surface,

similar to scanning electron micrographs. Scanning ion images were always obtained after TOF-SIMS images.

**Microscopy.** The essential components of a vertical illumination microscope (Olympus, Melville, NY) were used to capture reflected bright-field and epifluorescent images from samples mounted on the cold analysis stage of the TOF-SIMS instrument (Figure 1). We used 50-W halogen and 100-W Hg light sources. A Spot RT camera (Diagnostic Instruments, Sterling Heights, MI) using a cooled CCD and a tunable LCD filter was mounted onto the trinocular microscope head. The sample was viewed in real time, and bright-field or fluorescence pictures were captured in color or monochrome. For fluorescence studies of red fluorescent beads and DiI-labeled cells, an Omega (Battleboro, VT) XF101 filter set was used for selection of excitation and emission wavelengths (549 and 565 nm, respectively).

**Photobleaching of DiI.** For photobleaching experiments, a lipophilic membrane dye, DiI (Molecular Probes, Eugene, OR), was dissolved in ethanol (0.5 mg/mL). A micropipet bent in a U-shape to act as a small UV–visible transparent sample container was filled with the DiI solution. The micropipet was placed into

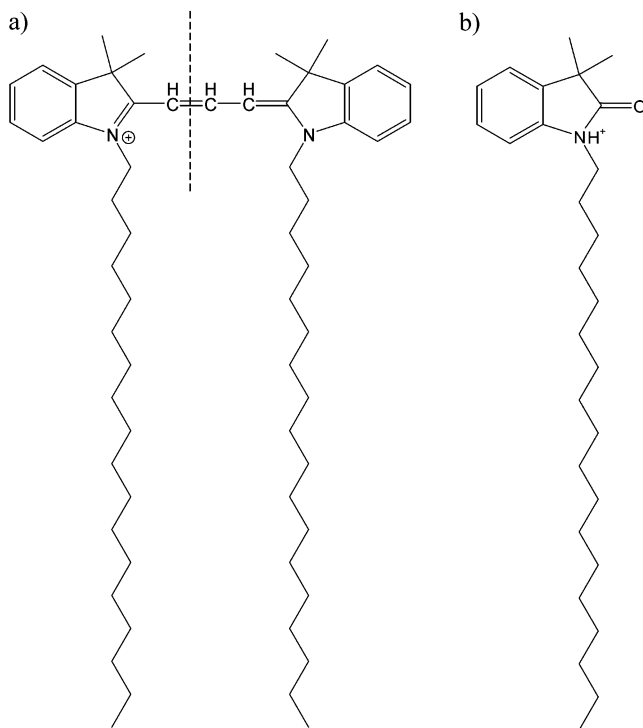


Figure 5. (a) Structure of DiI molecule with a line indicating an observed fragmentation that results in peaks between  $m/z$  410 and 424 and (b) ion resulting from hydrolysis of DiI with  $m/z$  414.

the path of a pulsed Nd:YAG laser (30 Hz, 6 ns, 532 nm, 2.5 W; Spectraphysics, Mountain View, CA) for 25 min. Samples of 100  $\mu\text{L}$  of photobleached DiI and standard solutions of nonphotobleached DiI were spin-coated at 3000 rpm onto 0.5 cm  $\times$  0.5 cm silicon wafers of 0.5-mm thickness for TOF-SIMS analysis.

**Standards and PC12 Cell Preparation.** Red fluorescent polystyrene beads (3  $\mu\text{m}$ ; Duke Scientific, Palo Alto, CA) were dried onto silicon shards to correlate imaging techniques. A  $[\text{C}_5\text{H}_9]^+$  molecule-specific image of the beads was obtained, followed by the correlating scanning ion, bright-field, and fluorescence images. PC12 cells were obtained from American Type Culture Collection (Manassas, VA) and cultured onto 5 mm  $\times$  5 mm Si wafers (Ted Pella, Redding, CA) coated with type I mouse collagen (Sigma, St. Louis, MO). Differentiation was induced by adding 100 ng/mL nerve growth factor (Sigma) to the media for 2 days.<sup>24</sup> The cells were stained for 2 h in a solution of 10  $\mu\text{g}$  of DiI/mL of media immediately prior to freezing. The media and excess dye were removed by rinsing several times with phosphate-buffered saline (D-8662, Sigma) containing 5- $\mu\text{m}$ -diameter polystyrene beads (Duke Scientific). The relatively small bead diameter was chosen to approximate the thickness of PC12 cells when cultured onto a collagen-coated substrate. A silicon shard was placed onto the wafer, and the entire assembly was frozen by plunging into liquid propane. The freeze-fracture methods employed after the sample was introduced to the ultrahigh vacuum were described previously in detail.<sup>19</sup> Briefly, the sample stub was anchored onto a  $\text{LN}_2$ -cooled stage at  $-196$   $^\circ\text{C}$ . This stage and sample were slowly warmed to  $-105$   $^\circ\text{C}$  (as described by Cannon et al.<sup>19</sup>), at which time the silicon shard was removed, exposing a

fresh surface of the sample for analysis. Next, the sample was cooled to  $-196$   $^\circ\text{C}$  and moved onto the  $\text{LN}_2$ -cooled sample stage for analysis.

**Image Alignment.** Bright-field and fluorescent images were captured normal to the surface, and scanning ion and TOF-SIMS images result in mirror images of the sample collected from an angled ion beam. To view similar regions of the sample from the same perspective, bright-field and fluorescence images were rotated, flipped, and cropped in Adobe Photoshop to match the scanning ion and SIMS images. Once a method was devised during the instrument alignment, it was used for all subsequent images.

## RESULTS AND DISCUSSION

**Four in Situ Imaging Techniques.** To compare information obtained with each of the four imaging techniques, a collection of fluorescent beads on silicon has been imaged (Figure 2). Prior to collecting images, a region of interest is selected by microscopic examination. TOF-SIMS images of selected ions are collected first, followed by scanning ion, bright-field, and fluorescence images. The resolution of the bright-field and fluorescence images is limited by the in vacuo lens chosen to accommodate the focal length constraints of the instrument while providing an adequate field of view. In addition, images must pass through a series of feed-through windows and a dichroic mirror before image capture. Finally, since images are collected from reflective surfaces using epi-illumination, blurred edges become apparent. Still, single 3- $\mu\text{m}$  beads can easily be deciphered in the bright-field, fluorescence, and scanning ion images; however, they are less clear in the  $\text{C}_3$  hydrocarbon ( $m/z$  42) SIMS image as a result of the small amount of molecule-specific signal detected at each pixel. Qualitatively, resolution in SIMS can be viewed as the difference in intensity between adjacent pixels, which is determined by the amount of signal obtained at each pixel.<sup>25</sup> The small sampling area (200 nm) and the poor ionization efficiency of the insulating bead material limit the number of secondary species observed at each pixel. Clearly, single beads can be identified in the TOF-SIMS image, and these experiments can be used to resolve adjacent features within the molecule-specific images.

Unlike the pulsed ion beam in static SIMS, the continuous ion beam used in scanning ion imaging can obliterate the molecular species of interest and can cause significant charging of the sample. The bead, indicated by arrows in Figure 2a and b, has moved during scanning ion imaging. The movement of the bead is a clear illustration of the charging and damage that the sample experiences with constant scanning of the beam in scanning ion imaging versus a pulsed beam in static TOF-SIMS. As a result, scanning ion images are always collected after static SIMS analysis to prevent damage or relocation of the species of interest at the surface of the sample. Bright-field microscopy provides a blurred view of particle location. Fluorescence microscopy results in a slightly better resolved image and is specific for labeled or natively fluorescent molecules, providing an added element of selectivity. Scanning ion microscopy provides high-resolution morphological information without any chemical specificity and results in damage to the sample surface. Although the resolution of TOF-SIMS in the bead sample is not as detailed as for the other techniques,

(24) Greene, L. A.; Aletta, J. M.; Rukenstein, A.; Green, S. H. *Methods Enzymol.* **1987**, *147*, 207–216.

(25) Winograd, N. *Anal. Chem.* **1993**, *65*, 622A–629A.

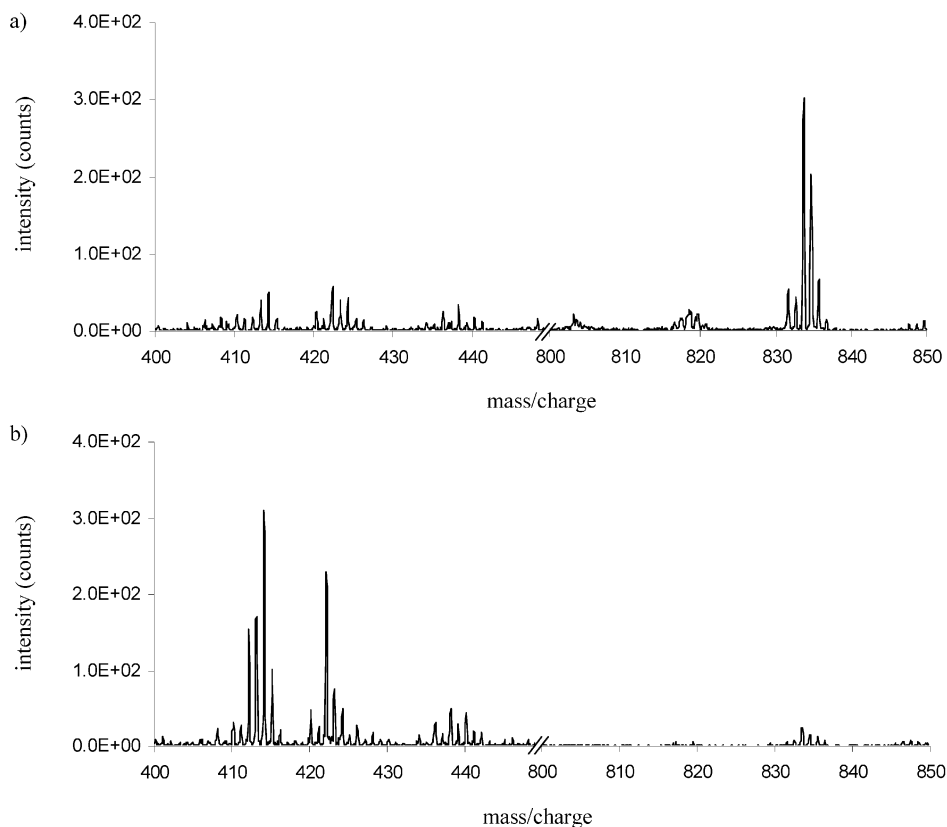


Figure 6. (a) Regions of positive ion TOF-SIMS spectrum of nonphotobleached DiI and (b) regions of positive ion TOF-SIMS spectrum of photobleached DiI with decreased molecular ion ( $m/z$  834) and increased fragments in the  $m/z$  410–424 region.

this approach provides unmatched chemical specificity as described in the sections below.

**Imaging PC12 Cells with Complementary Imaging Techniques.** Although cells in culture are relatively easy to identify with phase contrast microscopy in liquid media, this technique is difficult with frozen samples. Location of cellular membrane structures is complicated by patterns in the ice matrix on the smooth reflective SIMS substrate.<sup>13,19</sup> Small (12–15- $\mu\text{m}$  diameter) cells are also difficult to distinguish from the 5- $\mu\text{m}$  beads used to prevent crushing of the cells during sample preparation. Staining the cells with DiI allows their visualization in the ice matrix as well as discrimination between stained cells, beads, and other particles that might be present in the sample. In this experiment, both differentiated and undifferentiated PC12 cells have been imaged. Differentiated cells are slightly larger than undifferentiated cells (shown later) and form aggregates as shown in Figure 3. The bright-field image (Figure 3c) clearly shows a large aggregate and several smaller objects. In contrast, the fluorescence image (Figure 3d) only shows the aggregate of cells, indicating that the other objects are not membranous and are probably beads, identified by their size, shape, and density in the bright-field image (Figure 3c). Figure 3a shows a TOF-SIMS image of these cells. The phosphocholine headgroup is imaged at  $m/z$  184 and is overlaid on the image of water at  $m/z$  18–19. There is a clear correlation between the headgroup ion and the cell bodies of the PC12 cells. As expected, the neurites present in differentiated PC12 cells are attached to the substrate several micrometers below the plane of the cell and are therefore not exposed during freeze-fracture and subsequent imaging. In contrast to the

molecule-specific information acquired with SIMS, the morphology of this cell cluster can be examined with scanning ion microscopy (Figure 3b). This image reveals a cell outgrowth at the top but also demonstrates that many of the outgrowths and the beads have not been uncovered from the ice. The correlation of TOF-SIMS imaging with two-dimensional bright-field and fluorescence microscopy and three-dimensional scanning ion imaging is clearly advantageous in identifying cells following freeze-fracture.

**Mass Spectra of DiI.** Since DiI is used to label membranes for imaging, it is important to evaluate the mass spectrometry of this molecule. The fragmentation pattern of DiI has been determined with TOF-SIMS and compared to the spectra of native membranes. The positive ion spectrum shown in Figure 4 demonstrates that DiI yields an intense molecular ion detected at  $m/z$  834. In addition, the molecule is fragmented between the two conjugated ring systems as shown in Figure 5a. This results in peaks occurring in the mass spectrum between  $m/z$  410 and 424 that are important to DiI (vide infra). The structure of a hydrolysis product ( $m/z$  414) that also appears to form during sample preparation is shown in Figure 5b. Abstraction of methylene units from the long hydrocarbon chains on the DiI molecule results in most of the remaining fragments present in the spectrum.

In addition to fragmentation during primary ion bombardment, photobleaching of the dye occurs during fluorescence analysis. While focusing and capturing images of DiI-stained PC12 cells, the fluorescence intensity of the cells reduces over time. This could result from photodegradation of DiI, which would influence the spectrum of the molecule during subsequent cell imaging

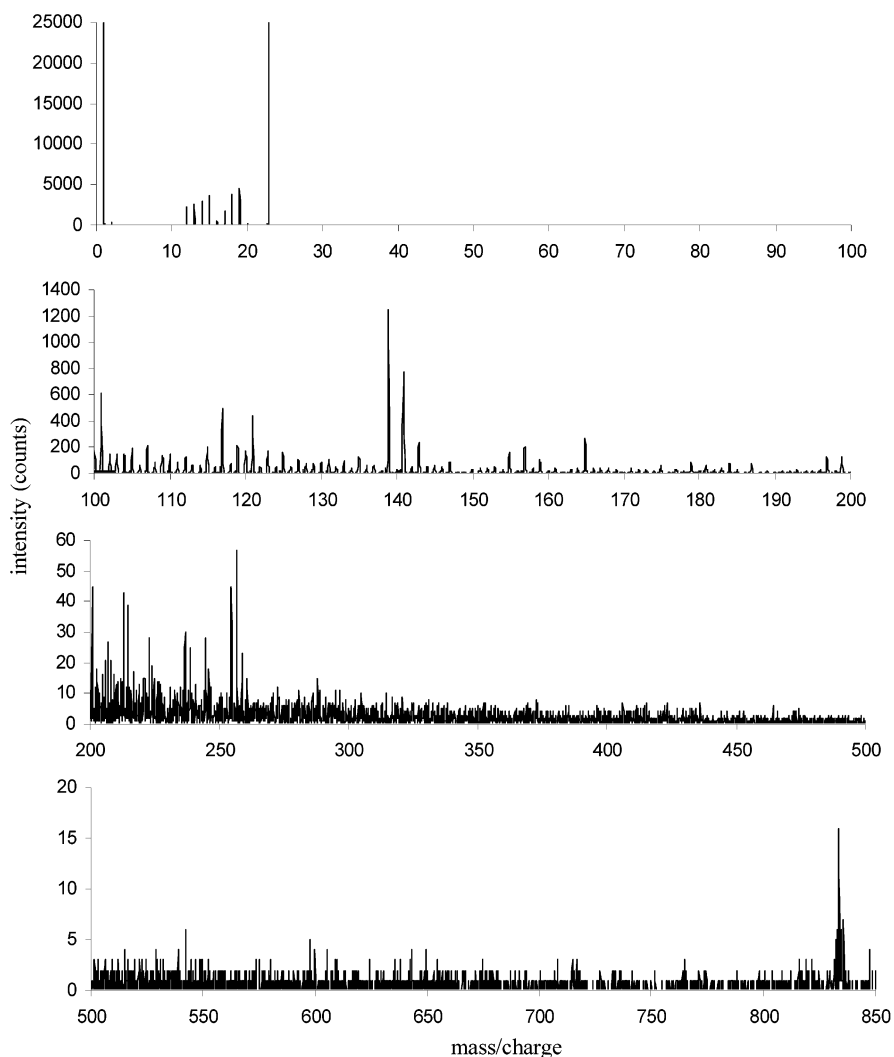


Figure 7. Positive ion spectrum of PC12 cell labeled with DiI. Peaks of interest include a hydrocarbon fragment  $[C_5H_9]^+$  at  $m/z$  69, phosphocholine at  $m/z$  184, a phosphocholine fragment at  $m/z$  86, cholesterol molecular ion at  $m/z$  386, and DiI molecular ion at  $m/z$  834.

experiments. To investigate this phenomenon, a solution of DiI in ethanol has been photobleached with the 532-nm line of a Nd:YAG laser. This wavelength mimics the region used in the fluorescence microscope (500–550 nm). The regions from  $m/z$  400–450 and 800–850 for photobleached samples are compared to nonphotobleached controls in Figure 6. The photobleached sample exhibits significantly less molecular ion and a greater amount of the fragment ions between  $m/z$  410 and 424. Although all fragment ions have not yet been identified, the mechanism of the photodegradation appears to involve cleavage of DiI near the center of the molecule. Thus, the spectra of both DiI and photobleached DiI contain significant peaks at  $m/z$  834 and in the region between 410 and 424. In addition, smaller mass spectral peaks are present for DiI fragments across the mass spectral region used in these experiments. Most notably, DiI fragmentation during SIMS results in minor peaks near  $m/z$  184, which corresponds to the phosphocholine headgroup ion. These fragment ion patterns must be considered when imaging labeled cell membranes with TOF-SIMS.

**TOF-SIMS of PC12 Cells.** As discussed above, fluorescence microscopy greatly enhances the ability to locate cells for TOF-SIMS analysis. A spectrum of a single undifferentiated PC12 cell

labeled with DiI is shown in Figure 7. In addition to the smaller ions of  $H_3O^+$  and  $Na^+$ , hydrocarbon fragments dominate the spectrum up to about  $m/z$  250. There are also smaller amounts of  $K^+$ , phosphocholine ( $m/z$  184), a phosphocholine fragment ( $m/z$  86),<sup>18</sup> cholesterol-OH ( $m/z$  369), and DiI ( $m/z$  834) that are found in the cell membrane. Previous experiments have shown phosphocholine as the dominant ion in TOF-SIMS analyses of membranes without DiI present.<sup>12,13,18,19</sup> Since DiI also has a peak in its spectrum at  $m/z$  184, the isotopic profiles of the DiI standard and of the cell have been compared to determine the effect of DiI fragments on the intensity of the phosphocholine peak in the spectrum. Figure 8 demonstrates a significant difference in the ratios of the  $m/z$  184 to 182 peaks in the spectra for the DiI sample versus the cell sample. This evidence suggests that ions detected at  $m/z$  184 in the cell sample are probably due to species such as phosphocholine.

Water, cholesterol, phosphocholine, the phosphocholine fragment, and a hydrocarbon fragment have been chosen for TOF-SIMS imaging of the membrane. Images of the phosphocholine headgroup and a phosphocholine fragment ion ( $m/z$  86) are compared to those for a C5 hydrocarbon fragment and for cholesterol in Figure 9. These are all overlaid on the background

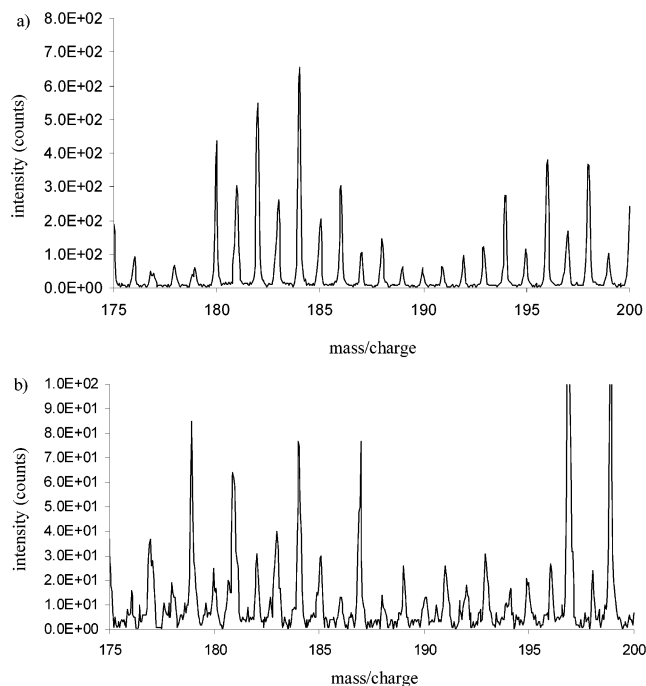


Figure 8. Region from  $m/z$  175 to 200 from spectra of (a) Dil and (b) a PC12 cell. The ratio of  $m/z$  184 to 182 in the cell sample is reversed from the Dil sample.

image of water. The presence of a cell is confirmed by the absence of water signal and the elevated intensity of C5 hydrocarbons. Localization of the membrane species occurs at the single-cell dimension of  $\sim 15 \mu\text{m}$  but also exists in small quantities outside the cell boundary, possibly due to lipids or collagen fragments in the surrounding aqueous media. As expected when the membrane is uncovered, the membrane species signal is in negative contrast to the water signal. The colocalization of the phosphocholine fragment at  $m/z$  86 with  $m/z$  184 is further indication that the  $m/z$  184 signal is due to phosphocholine present in the membrane of the PC12 cell. Furthermore, these images clearly demonstrate that the TOF-SIMS technique can be used to analyze phospholipids in single-cell membranes. Using combined fluorescence and TOF-SIMS, it is possible to locate a single PC12 cell in the freeze-fractured sample, obtain a spectrum of the region containing the cell, and image molecules of interest across the surface of the cell membrane. Further experiments will focus on expanding this integrative imaging analysis to investigate the molecular heterogeneity of other membrane lipids associated with cellular membrane function in single mammalian cells.

#### SUMMARY

Locating and imaging mammalian cells in the ice of frozen hydrated samples is challenging with bright-field microscopy and TOF-SIMS alone. The addition of in situ fluorescence microscopy

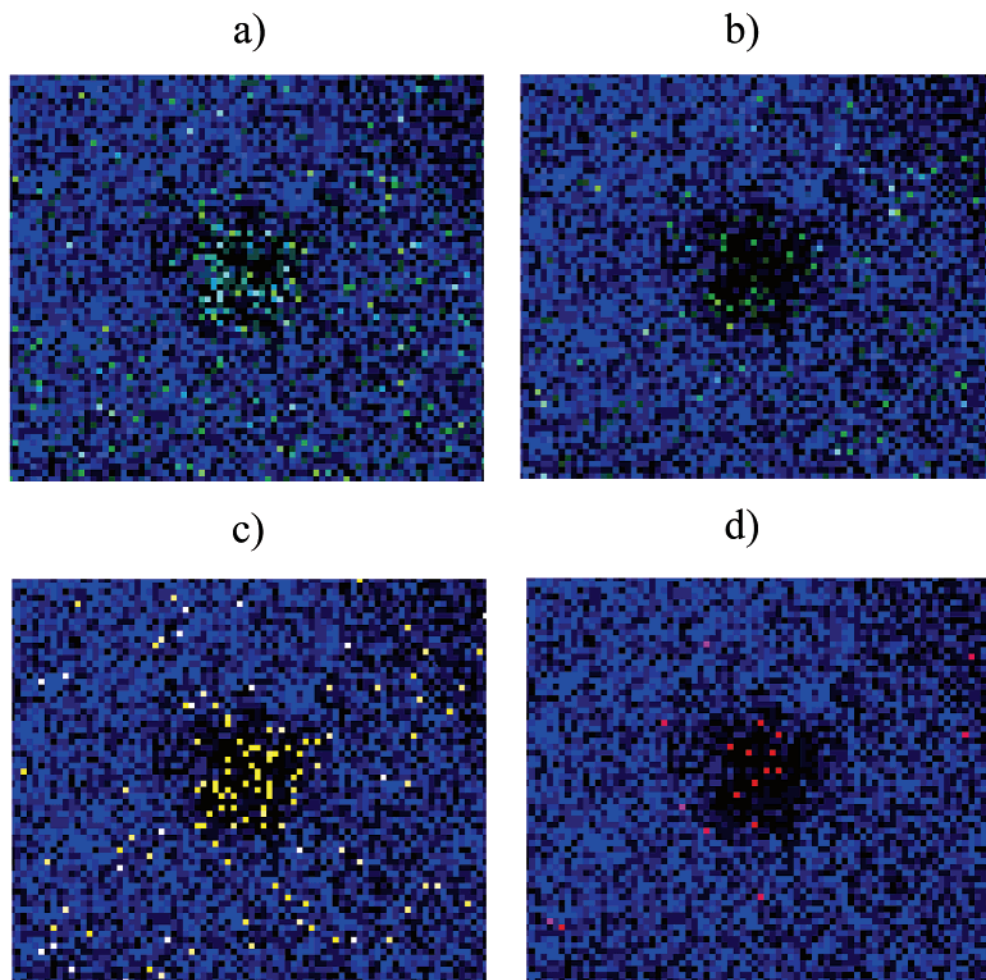


Figure 9. Positive ion molecule-specific images of freeze-fractured PC12 cells. Ions of interest are overlaid on water plotted as blue intensity on a 0–5 count scale. A  $50\text{-}\mu\text{m}$ -wide field of view: (a)  $m/z$  69  $[\text{C}_5\text{H}_9]^+$  on a 1–4 count scale, (b)  $m/z$  86 [choline,  $\text{C}_5\text{H}_{12}\text{N}]^+$  on a 1–4 count scale, (c)  $m/z$  184 (phosphocholine headgroup  $[\text{C}_5\text{H}_{15}\text{NPO}_4]^+$ ) on a 0–1 count scale, and (d)  $m/z$  369 (cholesterol-OH ion) on a 0–1 count scale.



makes it possible to locate fluorescently labeled cells in the ice of a sample prior to TOF-SIMS analysis. DiI has been used to label cell membranes prior to analysis and has been shown not to interfere with the TOF-SIMS imaging of native species in PC12 cell membranes. Scanning ion imaging has been used in addition to fluorescence and bright-field to provide information about the morphology of cells within a complex ice matrix. TOF-SIMS has been used in conjunction with these imaging techniques to study the chemical makeup of membrane components in single PC12 cell membranes. The combination of these imaging techniques with new methods for higher SIMS signal to study membranes of single cells will facilitate an understanding of the functional role of lipid domains in membranes on a molecular level.

#### ACKNOWLEDGMENT

The authors acknowledge support, in part, for this work from a grant from the NIH and acknowledge the National Science Foundation for continuing support of the instrumentation. The authors also thank Daniel Jones for his assistance in mass spectral interpretation and Jonathan Day for his assistance and expertise in the fluorescence imaging experiments.

Received for review February 8, 2002. Revised manuscript received May 27, 2002, Accepted June 18, 2002.

AC0255734